

# Demonstration and Comparison of GaN/Sapphire and InGaP p-i-n devices for Tritium Betavoltaic Power Source

30 September 2021

*Muhammad Khan (PI)  
Alexander Sweeney, (Branch  
Manager)  
and Oliver Barham, Ph.D*

Members of IHD E36 Branch

Marc Litz, PhD  
Randy Tompkins, PhD

Members of U.S. Army  
Research Laboratory SEDD

Agis Iliadis, PhD  
PhD Advisor  
ECE Department, University of  
Maryland, College Park

**DISTRIBUTION STATEMENT A (19-198): Approved for  
Public Release; Distribution Unlimited.**



This page intentionally left blank.

## REPORT DOCUMENTATION PAGE

*Form Approved*  
OMB No. 0704-0188

The public reporting burden for this collection of information is estimated to average 1 hour per response, including the time for reviewing instructions, searching existing data sources, gathering and maintaining the data needed, and completing and reviewing the collection of information. Send comments regarding this burden estimate or any other aspect of this collection of information, including suggestions for reducing the burden, to Department of Defense, Washington Headquarters Services, Directorate for Information Operations and Reports (0704-0188), 1215 Jefferson Davis Highway, Suite 1204, Arlington, VA 22202-4302. Respondents should be aware that notwithstanding any other provision of law, no person shall be subject to any penalty for failing to comply with a collection of information if it does not display a currently valid OMB control number.  
**PLEASE DO NOT RETURN YOUR FORM TO THE ABOVE ADDRESS.**

<b>1. REPORT DATE (DD-MM-YYYY)</b> 30-09-2021		<b>2. REPORT TYPE</b> Technical Report / Project Summary		<b>3. DATES COVERED (From - To)</b> FY21	
<b>4. TITLE AND SUBTITLE</b>  Investigation and Comparison of GaN/Sapphire and InGaP p-i-n devices for Tritium Betavoltaic Power Source				<b>5a. CONTRACT NUMBER</b>	
				<b>5b. GRANT NUMBER</b>	
				<b>5c. PROGRAM ELEMENT NUMBER</b>	
<b>6. AUTHOR(S)</b>  Muhammad Khan, Principal Investigator				<b>5d. PROJECT NUMBER</b>	
				<b>5e. TASK NUMBER</b>	
				<b>5f. WORK UNIT NUMBER</b>	
<b>7. PERFORMING ORGANIZATION NAME(S) AND ADDRESS(ES)</b>  NSWC - IH Division 4005 Indian Head Hwy, Indian Head, MD 20640				<b>8. PERFORMING ORGANIZATION REPORT NUMBER</b>  IHTR-2021-004010	
<b>9. SPONSORING/MONITORING AGENCY NAME(S) AND ADDRESS(ES)</b>  IH Division				<b>10. SPONSOR/MONITOR'S ACRONYM(S)</b>	
				<b>11. SPONSOR/MONITOR'S REPORT NUMBER(S)</b>	
<b>12. DISTRIBUTION/AVAILABILITY STATEMENT</b>					
<b>13. SUPPLEMENTARY NOTES</b>					
<b>14. ABSTRACT</b>  In this study, the performance of gallium nitride (GaN) and indium gallium phosphide (InGaP) semiconductor pin diodes designed for application as a tritium-based betavoltaic source is evaluated. Tritium is an attractive choice for a betavoltaic power source because it is inexpensive and least bio-toxic compared to other beta sources. Its average energy emission (5.6 KeV) does not cause lattice damage in most semiconductor crystals over its half lifetime of 12.5 years. We designed and fabricated betavoltaic devices on both sets of semiconductors and characterized them using a 6 KeV energy beam in order to evaluate their performance under a mean incident energy of a tritium beta source. Output powers of 160 nW and 101 nW with overall efficiencies of 8.88% and 5.62% were achieved for GaN and InGaP devices, respectively.					
<b>15. SUBJECT TERMS</b>  Betavoltaic Battery, Gallium Nitride (GaN), Indium Gallium Phosphide (InGaP), Tritium, Intrinsic layer, Depletion region, Semiconductor Junction					
<b>16. SECURITY CLASSIFICATION OF:</b>			<b>17. LIMITATION OF ABSTRACT</b>	<b>18. NUMBER OF PAGES</b>  29	<b>19a. NAME OF RESPONSIBLE PERSON</b>
a. REPORT	b. ABSTRACT	c. THIS PAGE			<b>19b. TELEPHONE NUMBER (Include area code)</b>

---

---

## **FOREWORD**

This work summarizes the efforts by the E36 Branch in developing a miniature, long life betavoltaic power source for sensors and low power electronics placed in remote (space, undersea, polar region, high mountains/desert, etc.) areas in order to enable capabilities that are not possible with current chemical batteries. New capabilities include decades-long lifetimes and operation in extreme hot/cold/shock environments. The work was sponsored Naval Surface Warfare Center (NSWC) Indian Head Division and supports the Ph.D. research of the Principle Investigator at University of Maryland, College Park. This report summarizes the Fiscal Year 2021 research effort.

Reviewed by:  
All Authors

Approved and released by:

---

---

## CONTENTS

<i>Heading</i>	<i>Page</i>
Forward .....	iii
Section 1: Introduction .....	1
Section 2: Betavoltaic Device Design and Operation .....	3
Section 3: Device Characterization and Discussion .....	11
Section 4: Conclusion .....	13
Appendix A: Fabrication Steps .....	16

## Figures

Figure 1: Schematic of a Betavoltaic Power Source. Beta Source is coupled to the top of a semiconductor PN or PIN junction. Beta particles create electron hole pairs in a semiconductor junction, which are then collected and provide power to an external load (not shown). .....	1
Figure 2: The maximum overall efficiency of a betavoltaic device as a function of material bandgap <sup>[3]</sup> .....	2
Figure 3: Bandgap representation of a betavoltaic device in operation.....	3
Figure 4: An example of an IV characteristics of a device in the dark and under beta illumination.....	4
Figure 5: Penetration depth of Tritium beta particles into InGaP = 500 nm (left) and GaN = 300 nm (right) .....	5
Figure 6: TCAD Simulation of the GaN/Sapphire Film Structure in the presence of an electric field. The u-GaN (i) layer thickness of 1 um with doping levels 1E16 results in an undepleted intrinsic region (not optimal design).....	6
Figure 7: TCAD Simulation of the GaN on Sapphire Film Structure in the presence of an electric field. The u-GaN (i) layer thickness is changed (reduced to 0.5 um from 1 um) and doping concentration of i-layer is not changed (still 1E16 cm <sup>-3</sup> ). This structure gives a fully depleted i-layer with an effective depletion region width of ~ 500 nm. ....	7
Figure 8: TCAD Simulation of the GaN/Sapphire Film Structure in the presence of an electric field. The u-GaN (i) doping concentration is changed (reduced to 1E15 from 1E16 cm <sup>-3</sup> ) and thickness of i-layer is not changed (still 1 um). This structure gives a fully depleted i-layer with an effective depletion region width of ~ 1 um.....	7
Figure 9: Maximum thickness of i-layer as a function of doping concentration of i-layer for optimized (fully depleted i-layer) performance. ....	8
Figure 10: GaN/Sapphire: Optical Image of a fabricated device (left) and Image of fabricated wafer with 4 devices, fully wirebonded and packaged for characterization.....	9
Figure 11: TCAD Simulation of the InGaP Film Structure in the presence of an electric field. The intrinsic (i) layer is doped at 1E10 cm <sup>-3</sup> and it is 10 nm thick. The thickness of the depletion region is 110 nm – the top n-layer is fully depleted. This structure is optimized for a solar cell device since photons carry much less energy and they penetrate far less into the material than beta particles.....	10
Figure 12: Image of a 6 inch fabricated InGaP wafer (right), Wirebonded and packaged InGaP ready for characterization (left).....	10
Figure 13: IV curve representing GaN device performance in the dark and under 6 Kev electron beam stimulus. Output power of 160 nW was calculated by multiplying voltage x current represented by red dot. ....	11
Figure 14.....	12
Figure 15: InGaP structure Optimized for Tritium Betavoltaics with a depletion region width (~ 700 nm) exceeding the penetration depth of tritium beta particles into InGaP.....	13

---

---

Figure 16: Fabrication etching step schematic .....	16
Figure 17: Fabrication metal deposition schematic.....	17

---

---

## ACRONYMS AND ABBREVIATIONS

3-H	Tritium
GaN	Gallium Nitride
InGaP	Indium Gallium Nitride
EHPs	Electron Hole Pairs

## SECTION 1: INTRODUCTION

### 1.0 Introduction

Betavoltaic power sources convert nuclear energy released in the form of beta particles directly into electrical energy. These power sources are needed for unattended sensors and other miniature low-power electronics for applications in remote (space, undersea, polar region, high mountains/dessert, etc) areas in order to enable capabilities that are not possible with current chemical batteries. New capabilities include decade-long lifetimes and operation in extreme hot/cold/shock environments. Chemical batteries dominate current battery technology and they work great for powering most commercial devices for short periods of time in favorable environment. However, they have limitations such as short life time and environment sensitivity (chemical rate is influenced by temperature) when it comes to powering devices in remote areas where the need is for decade of uninterrupted power in harsh (hot/cold/shock) environment. Betavoltaic power sources can overcome these limitations because beta decay is not a function of temperature or shock/vibration, therefore betavoltaic power source will produce power at the lowest achievable temperatures and when exposed to extreme shock/vibration. Betavoltaic power sources contain orders of magnitude of higher energy density (enables miniaturization into small, thin millimeter size package) compared to chemical batteries, and have long lifetimes (12.5 years with tritium). However, their main drawback is the low power density (low output power – 10's of  $\mu\text{W}/\text{cm}^2$ ). Therefore, they are ideal for devices requiring small amount of power over long periods of time such as unattended sensors, tagging/tracking devices and other miniature low power electronics placed in harsh environments.

Betavoltaic power sources consist of two main components: a beta source and a semiconductor junction (pn/pin diode) used to convert beta energy into electrical energy as shown in **Figure 1**

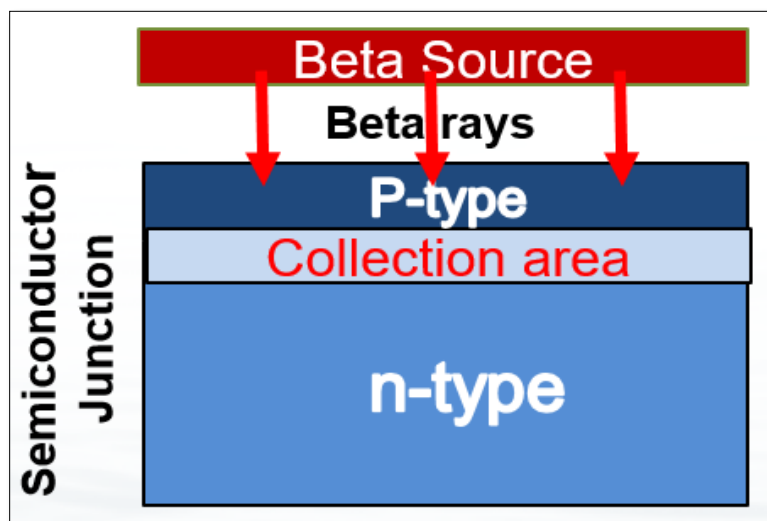


*Figure 1: Schematic of a Betavoltaic Power Source. Beta Source is coupled to the top of a semiconductor PN or PIN junction. Beta particles create electron hole pairs in a semiconductor junction, which are then collected and provide power to an external load (not shown).*

The principle of operation of a betavoltaic device is similar to a solar cell, except that electron hole pairs (EHP's) are created by beta particles instead of photons. Beta sources come in different energies ranging from a few KeV up to 15 MeV, and their half-lives from about a second to hundreds of years [1]. Semiconductors also come with narrow (0 – 2.1 eV), wide (2.1 – 3.4 eV), and ultra (> 3.4 eV) wide bandgap energies [2]. Theoretically, the efficiency of a betavoltaic device increases as the bandgap energy of the semiconductor is increased due to increase in higher open circuit voltage as shown in Figure 2 [3]. Wide bandgap semiconductors are more radiation hard (the atomic bond between atoms is much stronger) compared to narrow gap semiconductors, which potentially enables the use of high-energy beta sources such as Nickel-63, Promethium-147, and Strontium-90 to generate higher output power compared to low-power beta sources such as tritium. However, most wide bandgap semiconductors are not well advanced in terms of their growth, doping, and fabrication techniques, which limit their performance in a betavoltaic device so far. Commonly used narrow bandgap semiconductors do not suffer from such losses due to advancement made in their growth and fabrication techniques over the years. However, narrow bandgap semiconductors cannot be used with high-energy beta sources to generate higher output power/cm<sup>2</sup> because of the lattice damage due to high-energy beta particles.

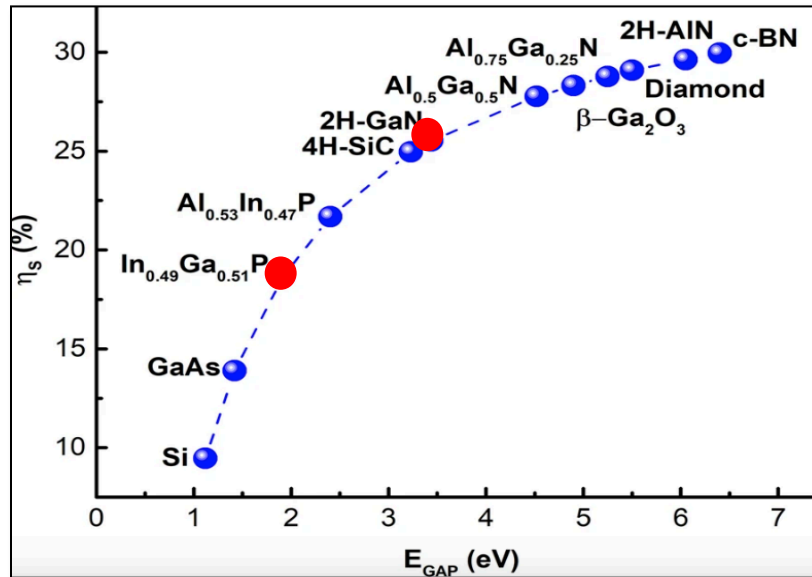


Figure 2: The maximum overall efficiency of a betavoltaic device as a function of material bandgap<sup>[3]</sup>

In this study, the performance of gallium nitride (GaN) and indium gallium phosphide (InGaP) semiconductor p-i-n devices designed for application as a tritium-based betavoltaic power source are evaluated. Tritium is an attractive choice for a betavoltaic power source because it is inexpensive and least bio-toxic compared to other beta sources. Its average energy emission (~6 KeV) does not cause lattice damage in InGaP and GaN semiconductor crystals over its half lifetime of 12.5 years. InGaP is a narrow bandgap semiconductor with an energy bandgap of ~ 1.9 eV with theoretical efficiency predicted to be around ~18 percent whereas GaN is a wide bandgap semiconductor with an energy bandgap of 3.4 eV with theoretical efficiency predicted to be ~ 26 percent as a betavoltaic device [3]. We designed and fabricated betavoltaic devices on both sets of semiconductors and characterized them using a 6 KeV

electron beam stimulus in order to evaluate their performance under a mean incident energy of a tritium beta source.

## SECTION 2: BETAVOLTAIC DEVICE DESIGN AND OPERATION

### 2.0 Betavoltaic Device Operation

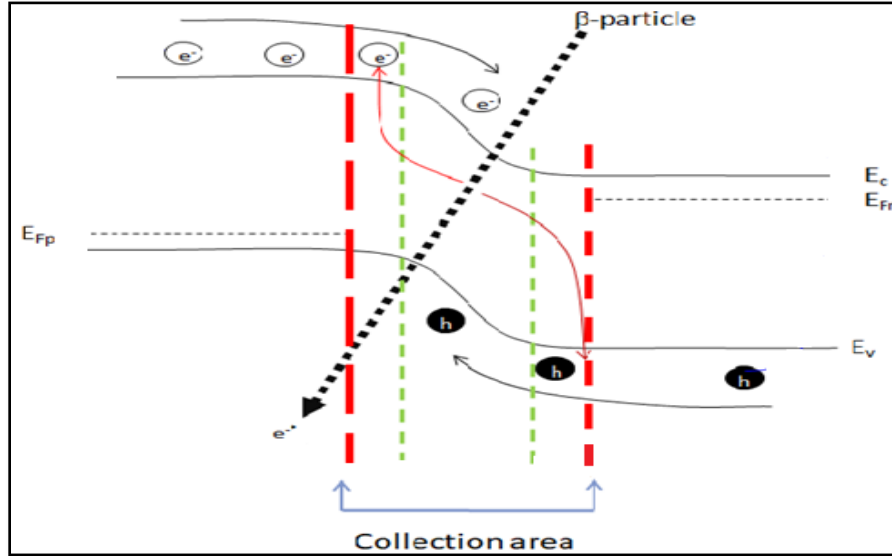


*Figure 3: Bandgap representation of a betavoltaic device in operation*

Figure 3 shows the representation of a betavoltaic device in operation. Beta rays incident on a semiconductor structure creates electron hole pairs (EHPs), which leads to external current/power. In a betavoltaic device, the equation for the current density is given by:

$$J = J_{sc} \left( e^{\frac{qv}{kT}} - 1 \right) - J_{\beta} \quad (1)$$

Where  $J_{\beta}$  is the current generated due to the result of incident beta particles. Since  $\beta$ -generated current density is negative, the I-V curve drops down into the 4<sup>th</sup> quadrant, which indicates the device is generating, as opposed to consuming, power. The current-voltage (I-V) characteristics of a betavoltaic device under beta irradiation (green curve) and under no irradiation (orange curve) are represented in *Figure 4*.

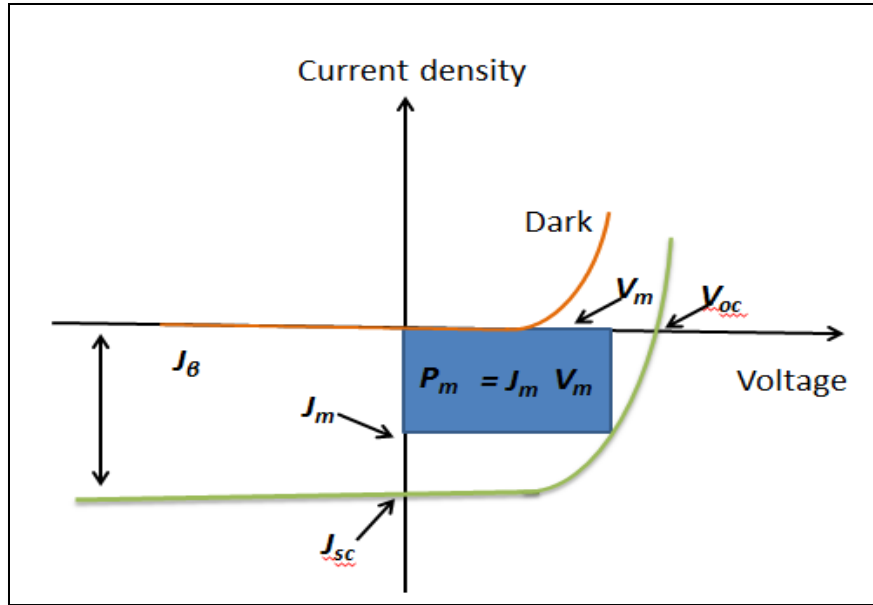


**Figure 4: An example of an IV characteristics of a device in the dark and under beta illumination**

When  $V = 0$ , the current is equal to short circuit current,  $J_{sc}$ , which is the same as  $J_{\beta}$ , and it is equal to  $V_{oc}$  when  $J_{sc} = 0$ . We want to maximize  $J_{\beta}$  but we have practically no control over how much of the beta particle's energy is converted into EHPs. This is dictated by the physics and it is  $\sim 35\%$  for most semiconductors [4]. However, we do have control over the number the electrons and holes that can be captured before they recombine. The efficient way to do this is to create EHPs in the depletion region where the probability of capture is almost 100% because there is an electric field that can sweep out the carriers to their respective terminals. EHPs that are created outside the depletion region simply recombine in the form of a photon or a phonon, and do not contribute to external current/power because there is no electric field outside this region.

A width of the depletion region is given by:

$$W = \sqrt{\frac{2\epsilon_s (N_a + N_d)}{q N_a N_d}} (V_{bi}) \quad (2)$$

Where:

$N_a$  and  $N_d$  are concentrations of acceptor and donor respectively.

$V_{bi}$  is the potential barrier seen by electrons and holes before diffusion and is given by:

$$V_{bi} = \frac{KT}{q} \ln\left(\frac{N_a N_d}{ni^2}\right) \quad (3)$$

The maximum power from the betavoltaic cell is obtained when the resistance of the load is selected such that it allows the current-voltage product to be maximized. The point at which this output power is maximized is called the maximum power point,  $P_m$  and can be expressed as:

$$P_m = J_m \cdot V_m \quad (4)$$

Where  $J_m$  and  $V_m$  are the peak current density and peak voltage points, respectively. The efficiency of a betavoltaic device ( $\eta$ ) describes its ability to efficiently convert incident beta electrons into electrical power. It can be described as the maximum power density delivered ( $P_m$ ) as a fraction of the incident beta power density from the radioactive source and can be expressed as:

$$\eta = \frac{P_m}{P_{in}} \quad (5)$$

Where  $P_{in}$  is the mean input energy from the beta source.

## 2.1 Betavoltaic Device Modeling

A semiconductor structure in the form of a P-i-N or N-i-P structure is used for a betavoltaic device. The purpose of the intrinsic (i) layer between P and N layers is to increase the width of the depletion region in order to maximize collection of carriers. The thickness and doping levels of i-layer are critical parameters (thickness is the function of doping levels) in determining the optimal width of the depletion region. In addition, it is important to determine the penetration depth of beta particles into the semiconductor junction so beta penetration range can be matched with the depletion region width to maximize collection of the EHPs.

We used MCNPX (Monte Carlo N Particle Transport) code to simulate how far beta particles penetrate into InGaP and GaN semiconductors for an average energy (6 KeV) emission of tritium beta source, as depicted in *Figure 5*.

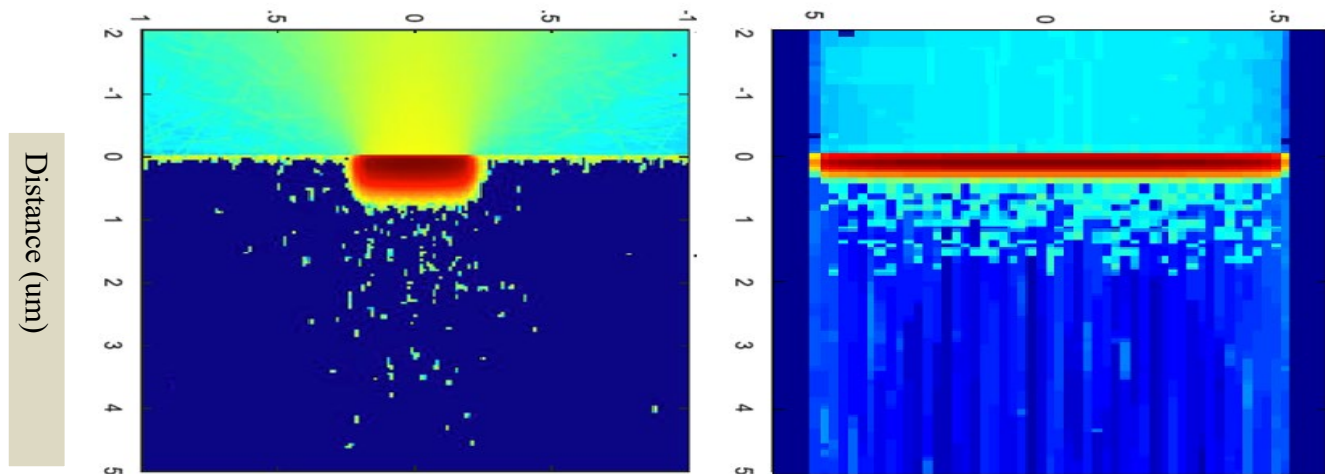


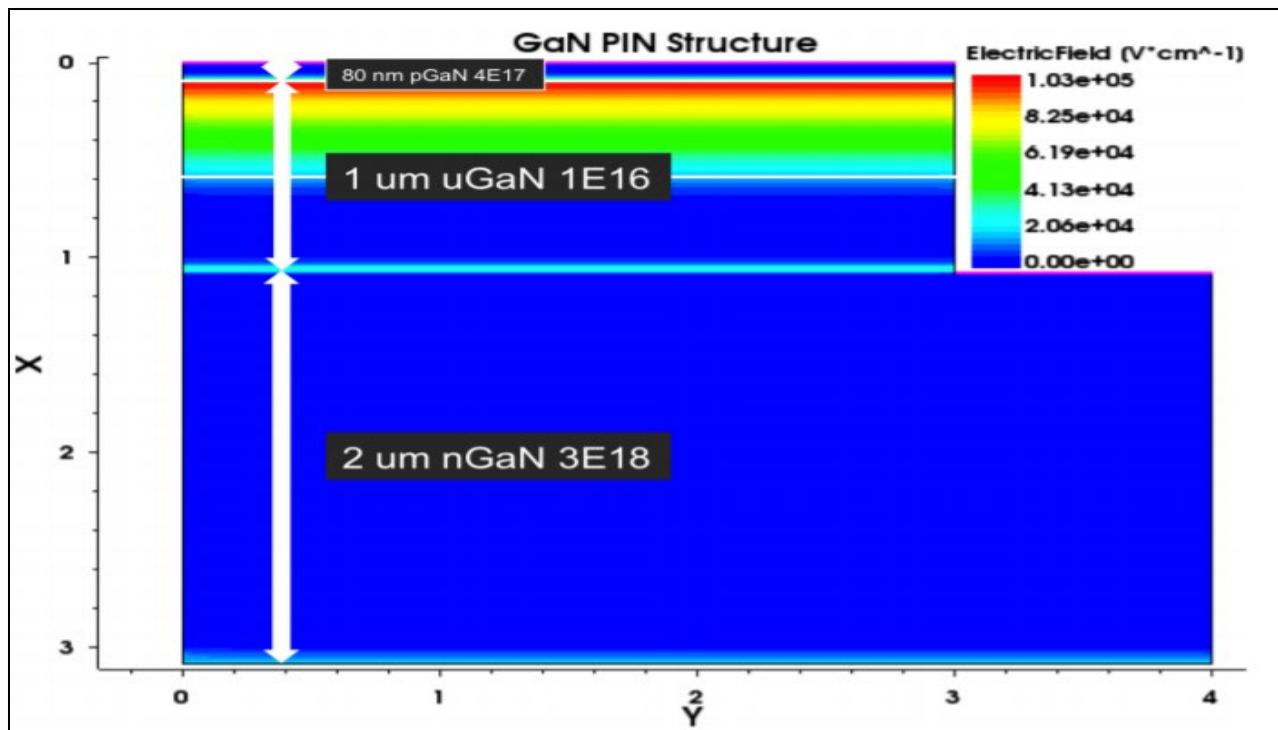
**Figure 5: Penetration depth of average (6 KeV) energy Tritium beta particles into InGaP = 500 nm (left) and GaN = 300 nm (right)**

The penetration depth of average energy beta particles from tritium penetrate 500 nm into InGaP and 300 nm into GaN semiconductor. Penetration depths are different for these two materials because their material

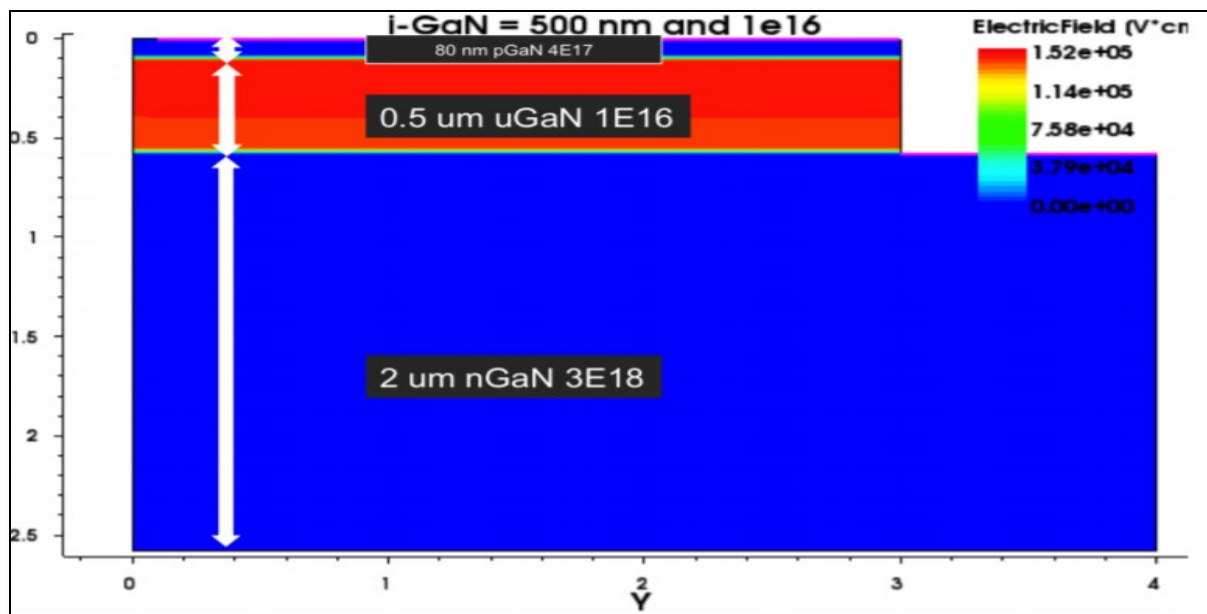
densities are different. For an optimized device performance, the depletion region needs to match or exceed this penetration depth in order to create maximum number of EHPs inside the depletion region where the probability of capture is 100 % due to the presence of electric field.

## 2.2 GaN Device

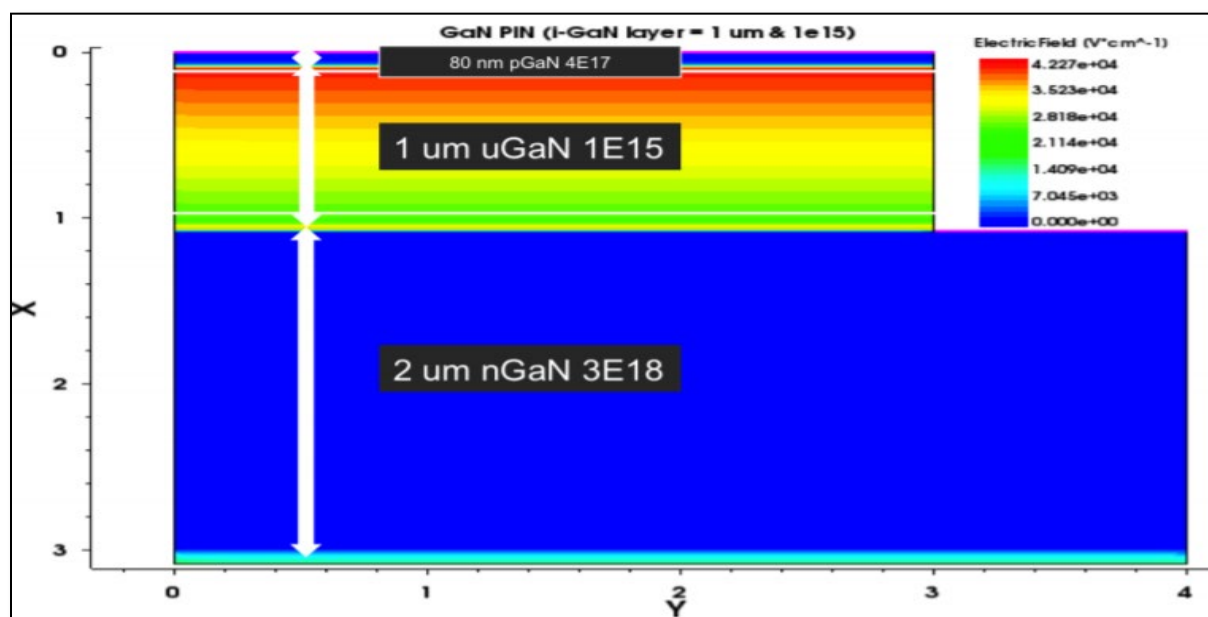
We used synopsys modeling to simulate different GaN p-i-n structures to determine an optimal design for a betavoltaic device. Figure 6 shows an example of a p-i-n structure that is not an optimal design because the i-layer (u-GaN) is not fully depleted between p & n layers. An un-depleted i-layer adds series resistance to the device, resulting in an inefficient device. Figure 7 and Figure 8 show two different structures that have a fully depleted i-layer (optimal designs).



*Figure 6: TCAD Simulation of the GaN/Sapphire Film Structure in the presence of an electric field. The u-GaN (i) layer thickness of 1 um with doping levels  $1E16$  results in an undepleted intrinsic region (not optimal design).*

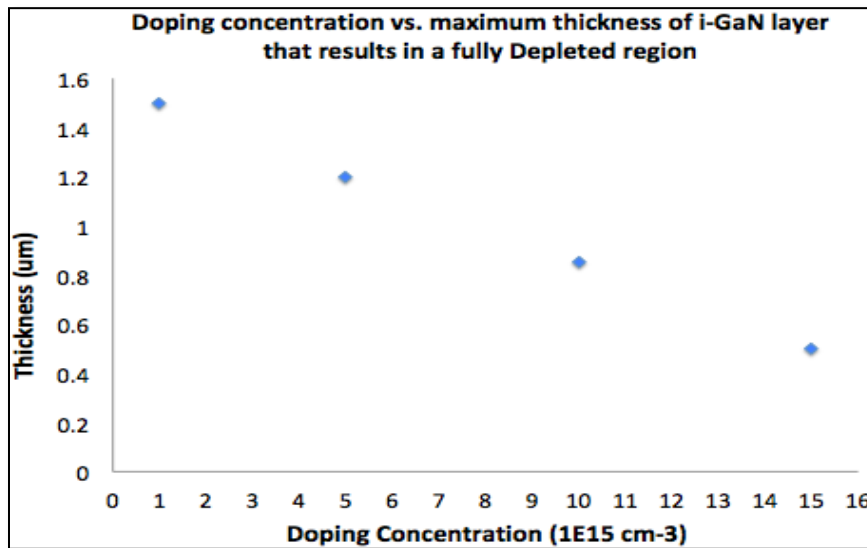


**Figure 7:** TCAD Simulation of the GaN on Sapphire Film Structure in the presence of an electric field. The u-GaN (i) layer thickness is changed (reduced to 0.5 μm from 1 μm) and doping concentration of i-layer is not changed (still  $1E16 \text{ cm}^{-3}$ ). This structure gives a fully depleted i-layer with an effective depletion region width of  $\sim 500 \text{ nm}$ .



**Figure 8:** TCAD Simulation of the GaN/Sapphire Film Structure in the presence of an electric field. The u-GaN (i) doping concentration is changed (reduced to  $1E15 \text{ cm}^{-3}$ ) and thickness of i-layer is not changed (still 1 μm). This structure gives a fully depleted i-layer with an effective depletion region width of  $\sim 1 \text{ μm}$ .

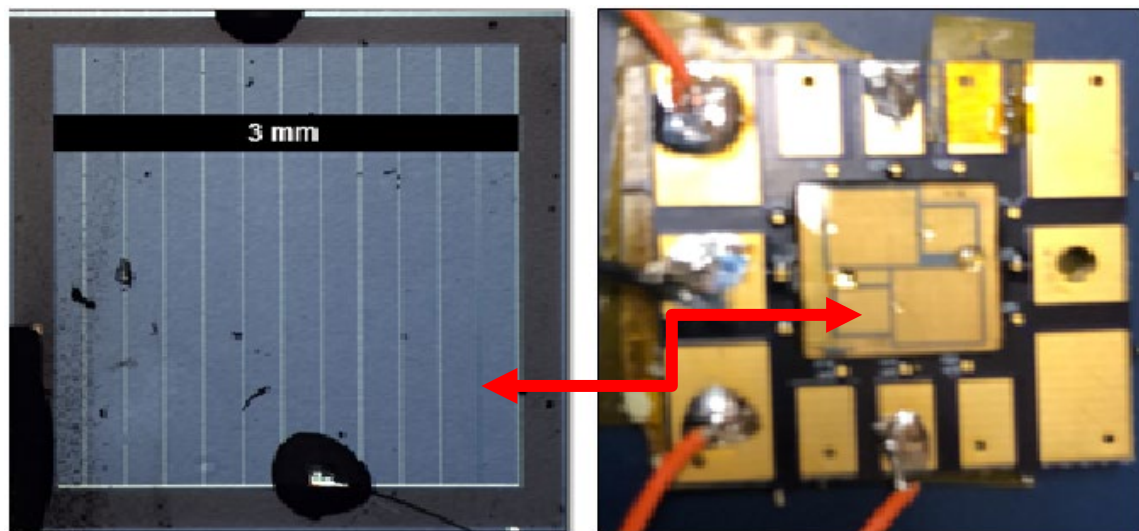
There are two ways to get a fully depleted i-layer between p and n layers, as depicted in Figure 7 and Figure 8. In a first method (Figure 7), only the thickness of the i-layer is changed from 1  $\mu\text{m}$  to 0.5  $\mu\text{m}$  and in the second method (Figure 8), only the doping concentration of i layer is changed (reduced to  $1\text{e}15\text{ cm}^{-3}$  from  $1\text{e}16\text{ cm}^{-3}$ ). Both these methods fully deplete the i-layer (optimal designs), but one method results in an effective depletion region width of  $\sim 500\text{ nm}$ , whereas second method results in an effective depletion region width of  $\sim 1\text{ }\mu\text{m}$ . Depending on beta source (penetration depth of beta particles into GaN) choice, one of these structures can be used to make an efficient GaN betavoltaic device. For example, we can use optimized structure in Figure 7 with tritium beta source since penetration depth of beta particles from tritium is only 300 nm. A depletion region width of 500 nm GaN device is sufficient to create and capture EHPs from tritium source. Similarly, i-layer thickness and doping concentration can be optimized for other beta sources depending on their beta particle energies and penetration depth. Figure 9 shows the maximum thickness of i-layer that is possible for each doping concentration that results in a fully depleted i-layer (optimal designs).



**Figure 9: Maximum thickness of i-layer as a function of doping concentration of i-layer for optimized (fully depleted i-layer) performance.**

Ideally, intrinsic layer is doped at  $1.5\text{E}10\text{ cm}^{-3}$  but this is not possible with GaN semiconductor due to doping challenges (n-type point defects) in its growth so far [5-6]. Currently, controllable doping levels of less than  $1\text{E}15\text{ cm}^{-3}$  are not possible for GaN semiconductor without compensation [5-6].

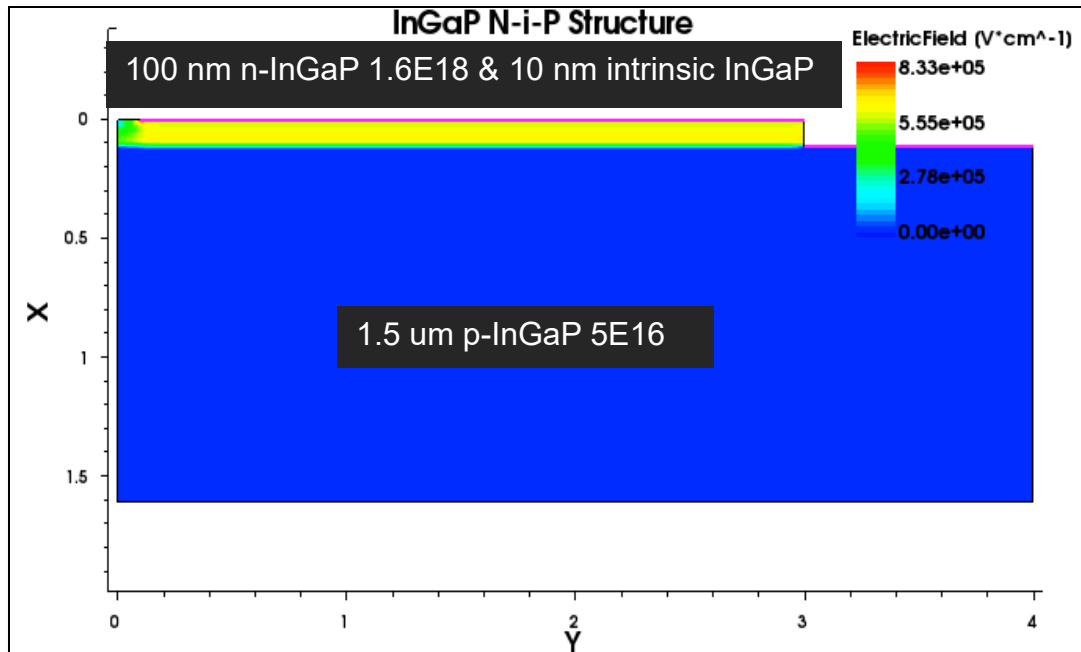
We fabricated (i-layer = 500 nm) structure in the cleanroom. The structure was commercially purchased, however the epitaxial layers were customized according to our specifications, as shown in figure 5. The major fabrication steps included photolithography and Inductive coupled plasma (ICP) etch to expose n-layer, evaporation of metal on positive and negative terminals, and wire bonding/packaging of the devices for characterization. Figure 10 shows an image of a fabricated and packaged GaN on sapphire devices.



*Figure 10: GaN/Sapphire: Optical Image of a fabricated device (left) and Image of fabricated wafer with 4 devices, fully wirebonded and packaged for characterization*

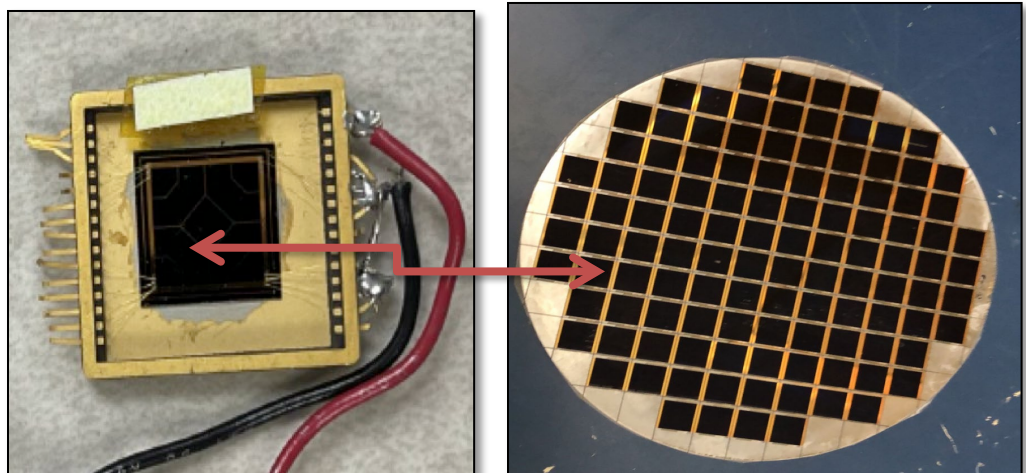
### 2.3 InGaP Device

Figure 11 shows the layer structure for the InGaP n-i-p structure. This structure was grown by Rochester Institute of Technology by 3×2" Aixtron close-couple showerhead metal organic vapor phase epitaxy (CCSMOVPE) [7]. This structure was designed and optimized for solar cell devices, but because the principle of operation of a betavoltaic device is similar to solar cells, we used this structure for betavoltaic devices to explore the possibility of using optimized InGaP cells for future betavoltaic devices. Even though, the intrinsic layer is only 10 nm thick but it is doped at  $1.5 \times 10^{10} \text{ cm}^{-3}$  (magnitudes of lower doping than GaN), there is electric field present in the whole n-region on top and in the intrinsic region, which gives an effective depletion region width of  $\sim 110 \text{ nm}$ .



**Figure 11:** TCAD Simulation of the InGaP Film Structure in the presence of an electric field. The intrinsic (i) layer is doped at  $1E10 \text{ cm}^{-3}$  and it is 10 nm thick. The thickness of the depletion region is 110 nm – the top n-layer is fully depleted. This structure is optimized for a solar cell device since photons carry much less energy and they penetrate far less into the material than beta particles.

The InGaP devices were fabricated using standard photolithography and metal deposition, similar to GaN/Sapphire devices. Figure 12 shows an image of a fabricated and packaged InGaP device.



**Figure 12:** Image of a 6 inch fabricated InGaP wafer (right), Wirebonded and packaged InGaP ready for characterization (left)

### SECTION 3: DEVICE CHARACTERIZATION AND DISCUSSION

Both GaN and InGaP devices were characterized using a Keithly Semiconductor analyzing system at room temperature. First, the measurements were made in the dark to determine the performance of these devices without beta illumination, and then under a 6 KeV electron beam stimulus in order to simulate their behavior for a tritium beta source.

#### 3.0 GaN on Sapphire Device Characterization

**Figure 13** shows the IV characteristic of a GaN device in the dark and under 6 KeV electron beam stimulus. The IV curve shows good diode behavior in the dark with a turn on voltage of  $\sim 0.4$  V. Turn on voltage is defined as a voltage at which a diode starts to conduct current. In the presence of 6 KeV electron beam stimulus, the IV curve dropped down to 4th quadrant, indicating power generation in the device. The maximum peak power is a product of maximum current and maximum voltage given by equation 3. The maximum voltage and maximum current were determined to be 0.40 V and  $-4E-07$  A, respectively. The maximum peak power was calculated to be 160 nW for this device with an efficiency of 8.88 %. Efficiency was calculated using equation 5, where  $P_{in}$  is 1.8  $\mu$ W from the electron beam.

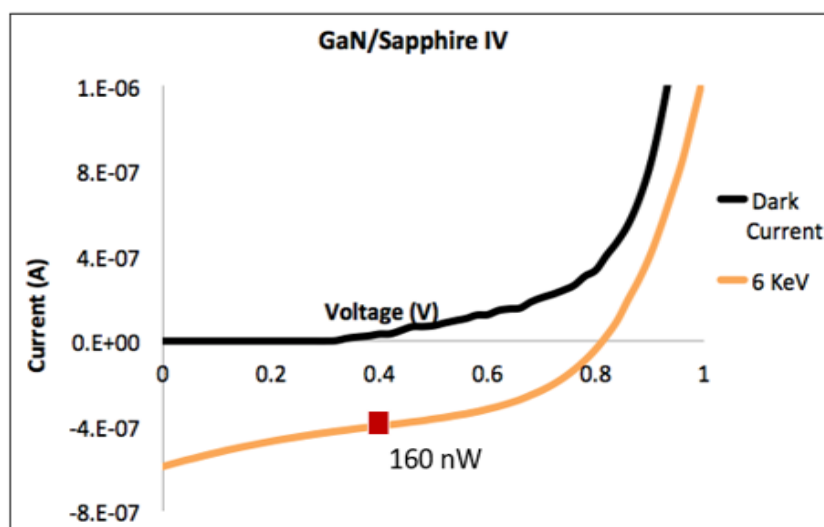


**Figure 13: IV curve representing GaN device performance in the dark and under 6 Kev electron beam stimulus. Output power of 160 nW was calculated by multiplying voltage x current represented by red dot.**

#### 3.1 InGaP Device Characterization

Figure 14 shows the IV characteristic of an InGaP device in the dark and under 6 KeV electron beam stimulus. The maximum voltage and current were determined to be 0.75 V and 1.35E7 A, respectively. We used equations 4 and 5 to calculate the power maximum and efficiency of the device,

respectively. The maximum voltage and current were determined to be 0.75 V and  $1.35 \times 10^{-7}$  A, respectively. The maximum peak power was calculated to be 101 nW with an efficiency of 5.62 %.

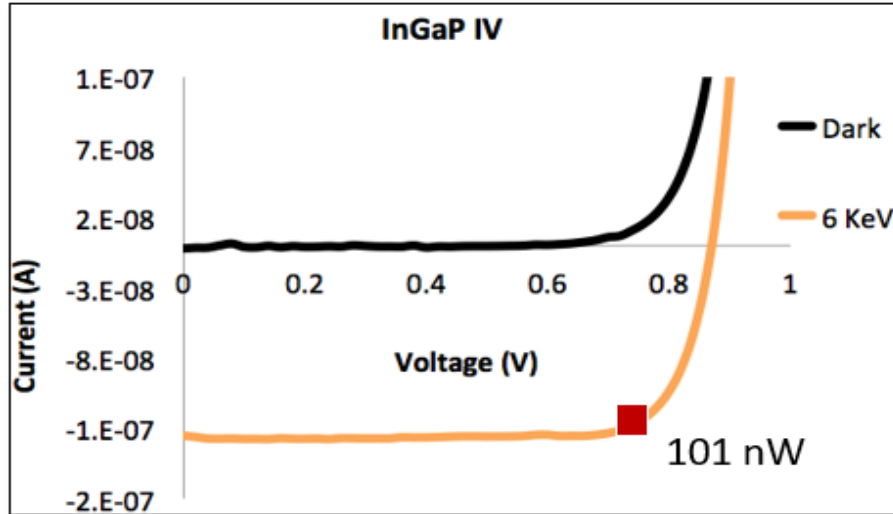


Figure 14

### 3.2 Discussion

GaN tritium betavoltaic device outperformed InGaP tritium betavoltaic device in terms of output power and efficiency. GaN device was designed and optimized to work as a betavoltaic device with a depletion region width of  $\sim 500$  nm. InGaP device was designed to operate as a solar cell and we used it as a betavoltaic device with a depletion region width of only  $\sim 110$  nm. From our MCNPX simulations, we determined that tritium beta energy is deposited 300 nm into GaN and 500 nm into InGaP semiconductor – this means we created most of the EHPs in the depletion region for a GaN device and only 22% ( $110/500$  nm) of EHPs for an InGaP device.

The GaN device was 3 x 3 mm in size whereas InGaP device was 10 x 10 mm in size. Given the size, the effective output power from GaN device is  $533 \text{ nW/cm}^2$  whereas effective output power from InGaP device is only  $101 \text{ nW/cm}^2$  when evaluated for a tritium betavoltaic power source. Open circuit voltage ( $V_{oc}$ ) was higher in InGaP device and short circuit current ( $J_{sc}$ ) was higher in GaN device, even though we expected both  $V_{oc}$  and  $J_{sc}$  to be higher in GaN device due to its wider bandgap. Given the results, there are areas for improvement in both InGaP and GaN devices. InGaP structure needs to be optimized for a betavoltaic device - to increase the width of the depletion region as depicted in figure 15. GaN device performance can be improved further by fabricating devices on a GaN film structure grown on a GaN substrate – to minimize dislocation defects. In this work, we fabricated GaN devices on GaN

film structure grown on a sapphire substrate – there is a 16 % lattice mismatch between sapphire and GaN which results in dislocation defects in the film structure.

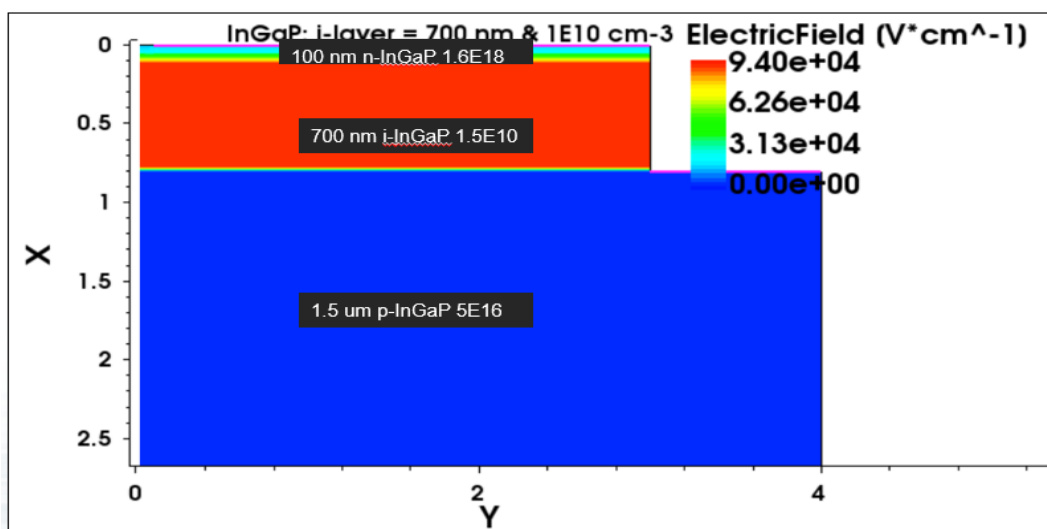


**Figure 15: InGaP structure Optimized for Tritium Betavoltaics with a depletion region width (~700 nm) exceeding the penetration depth of tritium beta particles into InGaP.**

Both GaN and InGaP are good choices for making a tritium betavoltaic power source. In terms of cost, InGaP device is inexpensive compared to GaN semiconductor. Also, InGaP wafers come in a 6-inch size whereas GaN wafer only come in 2-inch size so far – this saves time and money in fabrication.

#### SECTION 4: CONCLUSION

In summary, we have demonstrated a GaN p-i-n and InGaP n-i-p based devices operating as a tritium betavoltaic power source. GaN epitaxial layers were grown by MOCVD on a 2-inch c-plane sapphire substrate, InGaP devices were grown using CCSMOVPE. Devices were fabricated using standard photolithography and characterized using a 6 KeV electron beam in order to simulate their performance for a mean incident energy of a tritium beta source. Output power of 160 nW and 101 nW with overall efficiencies of 8.88 and 5.62 percent were determined at the average energy emission of tritium (6 keV) for GaN and InGaP devices, respectively.

### References

- [1] Lutz, Josef. "Pin-Diodes." *Semiconductor Power Devices: Physics, Characteristics, and Reliability*. Berlin: Springer, 2011. 159-66. Print.
- [2] Andreev V M, K E Bower, Y A Barbanel, Y G Shreter and G W Bohnert, *Polymers, Phosphors, and Voltaics for Radioisotope Batteries*, Boca Raton, FL: CRC Press, p 48 (2002).
- [3] Maximenko, S.I., Moore, J.E., Affouda, C.A. et al. Optimal Semiconductors for 3H and 63Ni Betavoltaics. *Sci Rep* 9, 10892 (2019). <https://doi.org/10.1038/s41598-019-47371-6>
- [4] C. Klein, *J. Appl. Phys.*, 39, 2029 (1968)
- [5] Cheong M G, *Appl. Phys. Lett.*, 77 2557 (2002)
- [6] Khan, R., Arora, A., Jain, A. *et al.* Impact of growth conditions on intrinsic carbon doping in GaN layers and its effect on blue and yellow luminescence. *J Mater Sci: Mater Electron* **31**, 14336–14344 (2020). <https://doi.org/10.1007/s10854-020-03993-5>
- [7] Y. Dai, H. Kum, M. A. Slocum, G. T. Nelson and S. M. Hubbard, "High efficiency single-junction InGaP photovoltaic devices under low intensity light illumination," *2017 IEEE 44th Photovoltaic Specialist Conference (PVSC)*, 2017, pp. 222-225, doi: 10.1109/PVSC.2017.8366547.

This page intentionally left blank.

**APPENDIX A: FABRICATION STEPS**

The major fabrication steps included:

1. Photolithography and ICP etch to expose n-layer
2. Evaporate metal (Ti/Al/Ni/Au) on the n-layer for negative terminal
3. Rapid Thermal Anneal (750°C, 30s)
4. Evaporate metal (Ni/Au) on p-layer for positive terminal
5. Rapid Thermal Anneal (500°C, 60 s)
6. Evaporate metal (Ti/Au) for wire-bonding and packaging

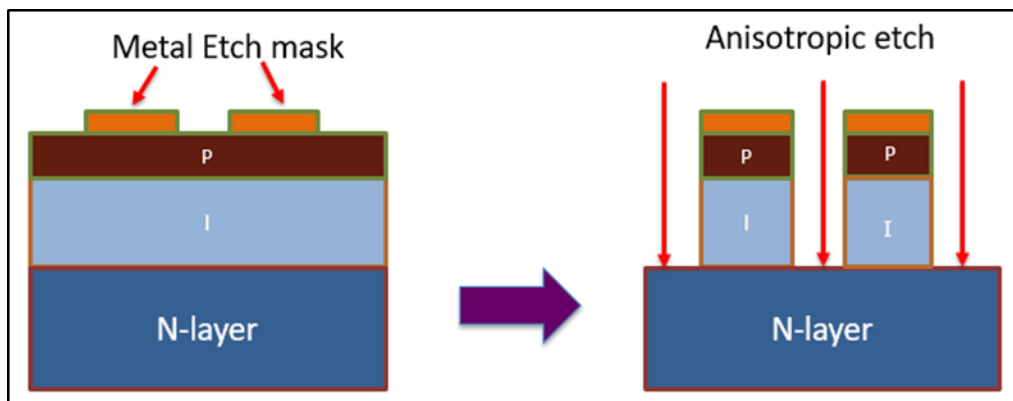


**Figure 16: Fabrication etching step schematic**

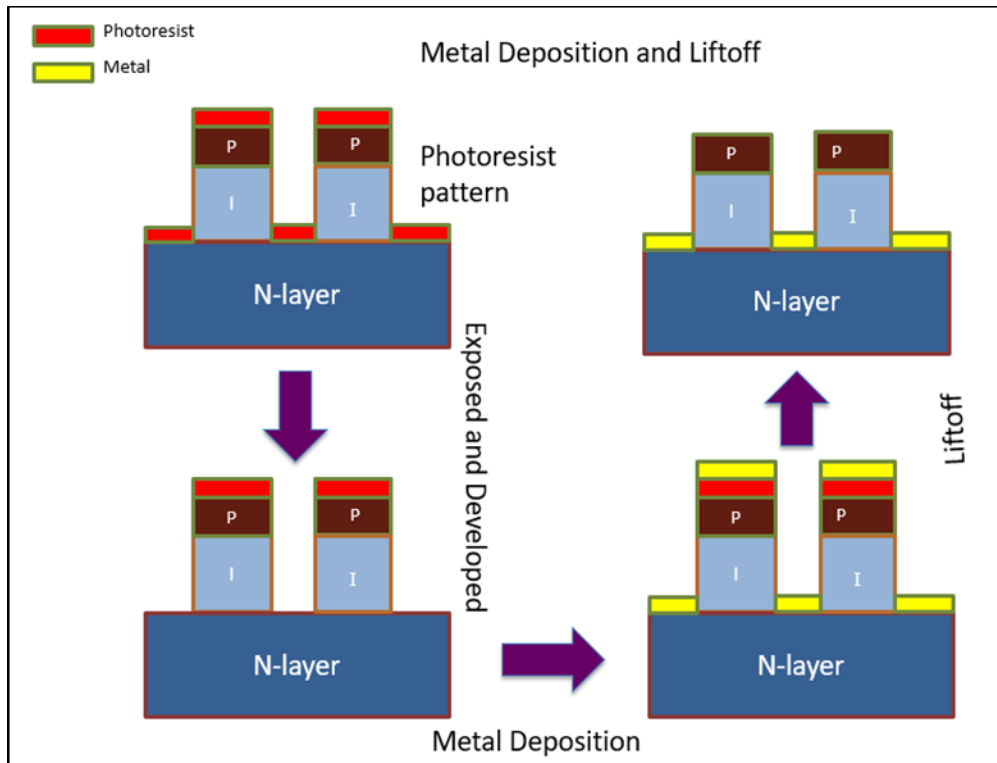


**Figure 17: Fabrication metal deposition schematic**

This page intentionally left blank





**DISTRIBUTION**

This page intentionally left blank.